

New Conformal PEC FDTD Model with User-Defined Geometric

Stefan Benkler¹, Nicolas Chavannes², and Niels Kuster¹

¹IT'IS Foundation for Research on Information Technologies in Society (IT'IS) - ETH Zurich, Switzerland

²Schmid & Partner Engineering AG (SPEAG), Zurich, Switzerland

INTRODUCTION

The most successfully used technique in electromagnetic (EM) computations is the Finite-Difference Time-Domain method (FDTD, Yee 1966). However, a well known deficiency is that the staircased meshing can lead to inaccuracies in the geometrical discretization of complex models. Conformal meshing and locally (near material interfaces) modified Yee update schemes can be used to overcome this deficiency. However, for the processing of complex simulation settings key issues such as the robustness of the conformal mesher and stability of the modified Yee scheme need to be addressed.

OBJECTIVES

The objectives of this study thus were the development and implementation of novel and robust 3-D CAD analysis algorithms for the fully automated generation of locally conformal FDTD meshes from arbitrarily complex geometries. Furthermore the additional geometric information is incorporated into the FDTD updating algorithm to achieve the same accuracy on a coarser grid, generating substantial savings in simulation time and memory consumption [2-4]. Finally, all schemes were integrated into the EM simulation platform SEMCAD X [5].

METHOD: CAD BASED GENERATION OF CONFORMAL FDTD MESHES

In particular for complex geometries, there is a strong need to automate the material property assignment to each computational cell. In the literature several attempts have been made (e.g., [6]) to use CAD data to extract the cell's material properties. The CAD data consists of a surface triangle description of the scenery to simulate. The result is a (conformal) object description of the scenery on the computational grid.

The addressed and presented problems are the algorithmic complexity and the handling of special cases as well as numerical difficulties with poorly shaped triangles. The difficulties are the same for staircasing and conformal discretization.

Overview of the Discretization

The grid lines are intersected with triangle mesh representing the object's surface. Each grid line thus knows if and where the object is hit. With the very efficient scan line conversion algorithm (computer graphics, Figure 4) all necessary data (dielectric staircasing voxels, staircasing PxC voxels, conform voxels) can be extracted out of these hit-points (called entry and exit point).

Tolerances and Special Cases

The intersection calculation of a grid line with poorly shaped surface triangles can lead to significant numerical errors. The calculation is therefore performed with tolerances, e.g., with a tolerance strip around the triangle (see surface triangle in figure 5).

An additional benefit of the tolerance strip is to avoid distinguishing between different cases when the grid line is tangential to the surface triangle. In the literature (e.g., [6], virtual gridlines) it is distinguished between the cases depicted in Figure 5. The tolerance strip enables easy but symmetric and robust discretization without differentiating special cases. The algorithm only investigates the entry/exit point pattern.

Examples & Benchmarks

The capabilities of the conformal FDTD mesh generator have proven its general versatility in a wide range of real-world applications. In Figure 2 a human model (head, hand) and mobile phone is shown, modeling the real-world situation of a phoning person. Figure 3 demonstrates the complexity of single parts of a commercial mobile phone model (antenna and case). Figure 1 shows a very detailed hearing aid model.

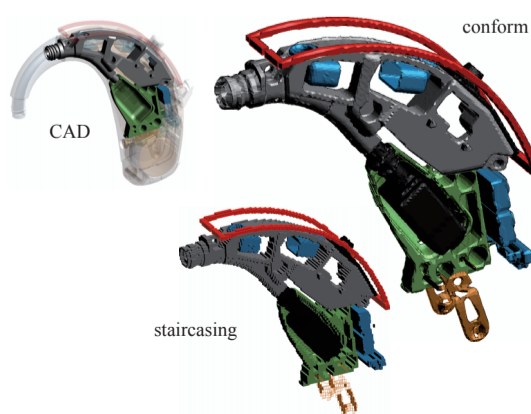


Figure 1: CAD representation, staircasing and conformal discretization of a commercial hearing aid with more than one hundred subparts, a grid of 49x130x145, approximately 200000 surface triangles, conformally voxelized in 12 seconds on a P4, 2.8GHz.

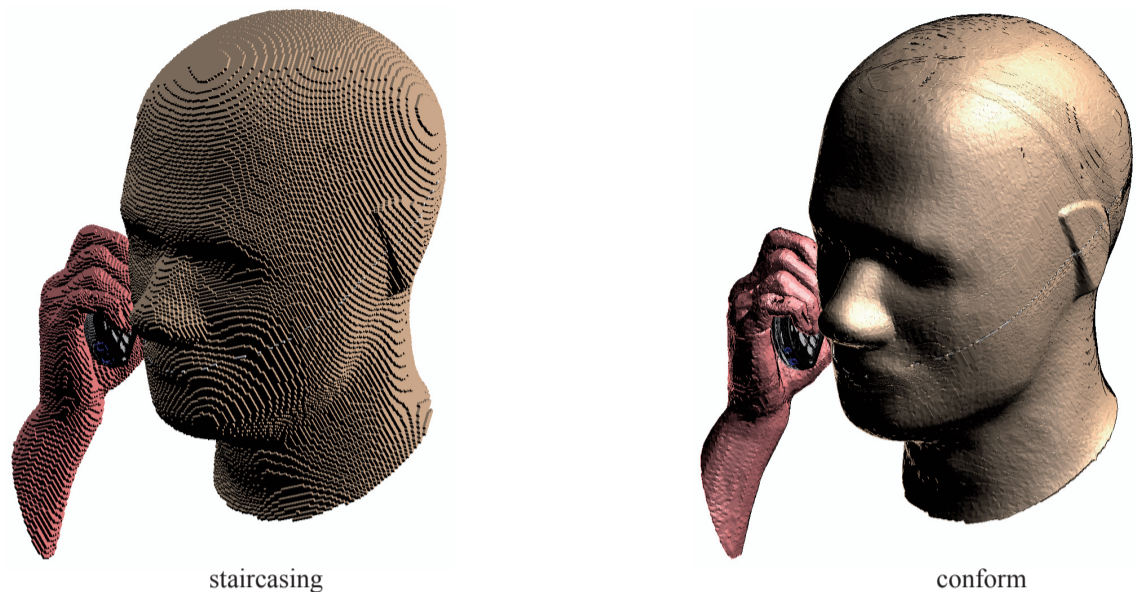


Figure 2: Staircasing and conformal discretizations using the same mesh sizes: SAM head, hand and mobile phone

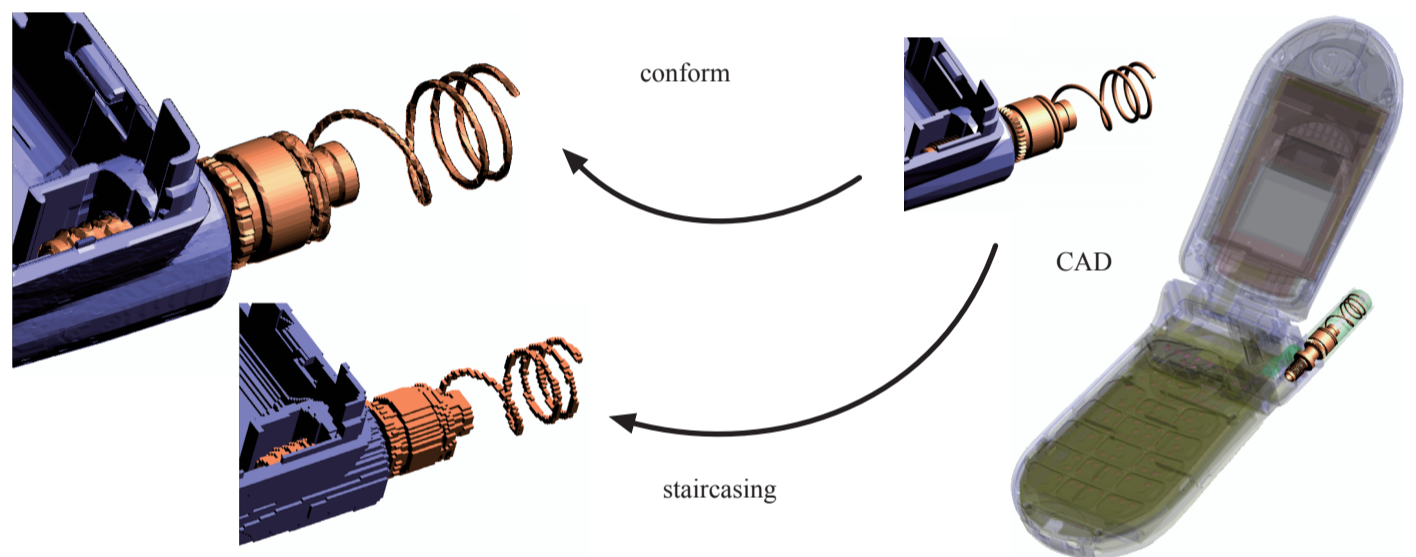


Figure 3: CAD representation, staircasing and conformal discretization of a commercial mobile phone with more than one hundred subparts, a grid of 166x426x186 and approximately 250000 surface triangles, conformally voxelized in 80 seconds on a P4, 2.8GHz.

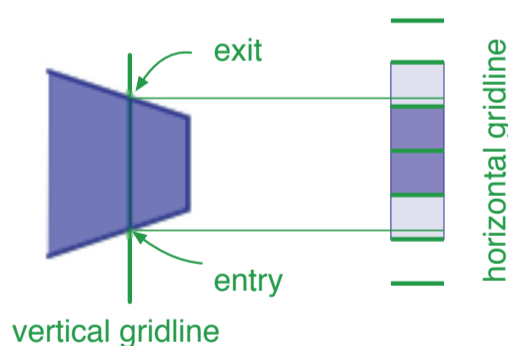


Figure 4: Scan conversion algorithm: the entry and exit points of an object hit by a grid line define the cells which are completely (dark blue) or partially (light blue) inside the object. Regardless of how many cells are between the entry and exit points, this kind of assignment scales according to the surface size instead of the object's volume size and thus the complexity is reduced. The technique can be used to assign a cell to its object, an edge to its object or a cut pattern of a conformal cell.

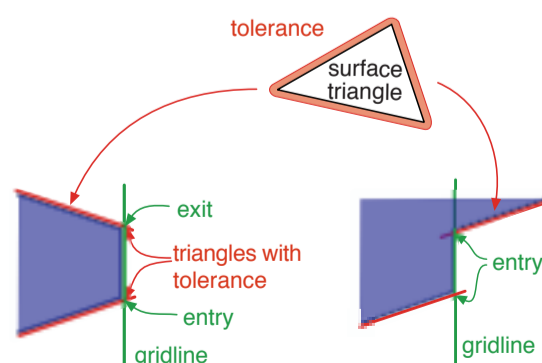


Figure 5: In the literature (e.g., [6]) it was reported that the two cases depicted in this figure needed to be handled differently. With a tolerance strip around the triangle (red) this problem is easily solved by looking at the entry/exit point pattern. If two entry points are in the list, then only the first one is considered; if an exit point follows, all is fine. The technique is symmetrical and robust, and no special treatment is necessary. Furthermore the numerical inaccuracies are overcome without any additional effort.

METHOD: CONFORMAL FDTD

The conformal discretization described in the first section is the basis for conformal FDTD simulations. The additional geometric information is incorporated into the FDTD algorithm to reduce the material assignment based error while keeping the spatial resolution and its corresponding errors. In the literature several attempts have been made to enhance accuracy [2,3,4].

The cited methods enhance the accuracy considerably; however some important details require improvement:

- modifications of the update stencil, e.g., split curl-coefficients (see equation (1))
- more multiplications per time step than conventional FDTD updating
- higher memory consumption than the conventional FDTD updating
- stability criterion: only guidelines based on experiments

A new conformal FDTD method [7] has been derived which overcomes these limitations.

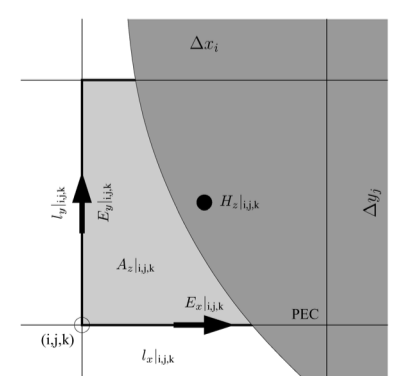


Figure 6: A loop for Faraday's law using the conventionally staggered grid. The lengths and area are the metal free parts.

Proposed Updating Scheme

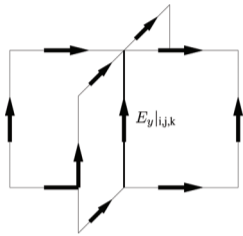
In every conformal FDTD algorithm the magnetic field update is modified according to Faraday's law in the following way (commonly used staggered FDTD grid notation [1]):

$$(1) \quad H_z^{n+1/2}|_{i,j,k} = H_z^{n-1/2}|_{i,j,k} + \frac{\Delta t}{\mu \cdot A_z|_{i,j,k}} \cdot (E_x^n|_{i,j+1,k} \cdot l_x|_{i,j+1,k} - E_x^n|_{i,j,k} \cdot l_x|_{i,j,k} - E_y^n|_{i+1,j,k} \cdot l_y|_{i+1,j,k} + E_y^n|_{i,j,k} \cdot l_y|_{i,j,k})$$

where E and H denote the electric and magnetic fields, Δt is the time step, n denotes the time step index, i, j, k are the spatial indices, μ denotes the permeability, and l and A are the PEC free length and area, respectively. This equation is used directly in the Dey-Mitra PEC model [2] (the conventional curl-coefficient ($\Delta t/\mu$) is split into four coefficients).

Same E-Field Prefactor

Considering a single electric edge E_y and all cell faces containing that edge the conformal FDTD equation (1) always describes the same prefactor l . Storing the product E_y times l_y instead of simply E_y avoids the split coefficients.



Modifications to Conventional FDTD Update

To recover the conventional FDTD time update equations the following modifications needs to be applied

$$\tilde{\mu} := \mu \cdot A_{\text{ratio}} \quad \tilde{\beta}_E(\Delta t) := \beta_E(\Delta t) \cdot \Delta_{\text{ratio}}$$

where β_E is the conventional FDTD coefficient in front of the curl of the H field.

Speed Versus Accuracy

A big advantage of the proposed conformal FDTD algorithm is that a time step reduction can be mathematically derived:

$$(2) \quad \Delta t_A^{\text{PEC model}} = \sqrt{\frac{A_A^{\text{ratio}}}{\max_{\text{edge} \in A} \Delta_{\text{ratio}}^{\text{edge}}}} \cdot \Delta t_A$$

where Δt_A is the conventionally calculated time step of that area A . The limiting factor in equation (2) is the reduced area A . Solving equation (2) for A_A^{ratio} and setting an acceptable time step $\Delta t_A^{\text{PEC model}}$, results in the lowest limit of A_A^{ratio} . If this limit is larger than the true area reduction, then the true area is increased to this limit to guarantee stability. Furthermore, the user has the possibility to favor either speed or accuracy depending on the acceptable timestep.

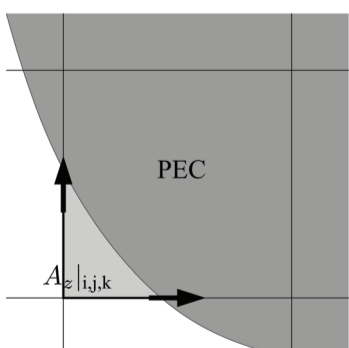
Optimal Timestep

The proposed scheme optimally connects a given time step with the achievable geometric precision:

1) *Nonuniform Grid*: On nonuniform grids the conventional local time step of cell faces can vary a lot throughout the grid. Therefore, a conformal coarse cell can incorporate a larger decrement of the conventional local time step and still satisfies the global time step. Hence, without any drawback a coarse cell can be conformally resolved more accurately than a smaller cell.

2) *Different Surrounding Dielectrics*: If the metal object is touching two different dielectrics, the dielectric with the larger permittivity has again a larger conventional local time step for the same cell size. Therefore, it is again conformally resolved more accurately with the presented scheme than the cells with the dielectric with the smaller permittivity.

3) *Small Largest Dielectric Edge Length in Cell's Face*: The case of a small area fractions below is considered:



Even if the cell is the smallest of the grid and the time step is not reduced (CFL = 1), the area A_A^{ratio} can be decreased (YM [3] uses always $A_A^{\text{ratio}} = 1$) because the maximal metal-free edge ratio $\max \Delta_{\text{ratio}}^{\text{edge}}$ is less than one (see equation (2)). Again the best geometric precision for a given time step is used in that cell.

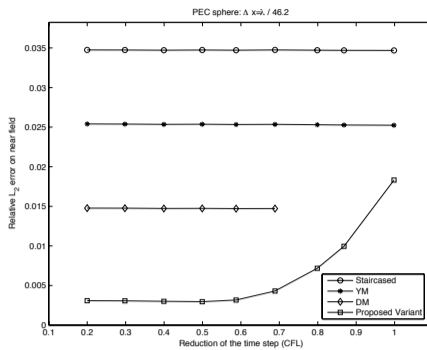


Figure 7: L_2 near field error on a grid $\Delta x = \lambda/46.2$. The scheme presented here shows that the user can tradeoff speed versus accuracy with the chosen CFL number. The improvements of the conformal FDTD method compared to the conventional one are obvious. The YM [3] scheme improves the accuracy compared to the staircased solution. However the proposed scheme with CFL = 1 can profit more from small cells. Using the DM [2] scheme, the accuracy can be improved even more. However, it suffers from example dependent late time instabilities. The presented scheme profits the most of the timestep reduction.

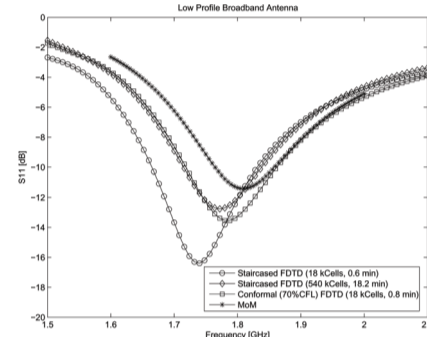


Figure 9: The conform FDTD on the coarse grid simulation gives a return loss which can be achieved only on fine staircasing simulations: the same accuracy is achieved with conventional FDTD method (18.2 minutes on an Intel P4, 2.7 GHz, 540 000 cells) as with the conformal one (70% CFL, 0.8 minutes, 18'000 cells)

NUMERICAL RESULTS & BENCHMARKS

In this Section the robustness and effectiveness of the proposed scheme is demonstrated on the basis of canonical validations as well as real world applications with increased complexity.

Benchmark 1: Validation With Mie Scattering

To outline the effect of the time step reduction and therefore the tradeoff of accuracy versus speed, the near and scattered fields of a metal sphere irradiated by an incident plane wave were investigated. The analytical solution is calculated by Mie series. The discrete norm L_2^2 (square root of the mean value of squared differences) was used to compare the simulated E field to the analytical solution. The near field region (box) has a side length 1.21λ (= 14 cells for the coarsest mesh) around the sphere center. The sphere's radius is $\lambda/5.77$ (= 2 cells for the coarsest mesh). The relative errors of near field and scattered field on different grids were subsequently investigated (Figure 7).

Benchmark 2: Low Profile Antenna

The next benchmark consists of the broadband low profile antenna Figure 8. A circular patch of 21 mm radius is located at 10 mm above a ground PEC plane. Two 10 mm off-centered metal rods of 1 mm radius short the patch with the ground plane. The antenna is excited at the center metal cylinder (radius 2 mm) with an edge source and a 1 mm gap between the cylinder and the ground plane (see also Fig. 5). The excitation signal was a sinusoidal Gaussian with a center frequency of 2 GHz and a bandwidth of 1 GHz. In Figure 9 the return loss is shown. The reference solution is based on method of moments (MoM). A significant improvement is achieved by conformal FDTD method with respect to both memory consumption and simulation time.

Benchmark 3: Mobile Phone

Whereas the previous benchmarks mainly focus on analysis of accuracy and efficiency of the proposed scheme, this section shall outline its robustness with respect to highly complex configurations, e.g., CAD derived devices. In addition, to also demonstrate its wide application range, a model of a commercially available mobile phone was chosen and simulated at 1.85 GHz. The CFL reduction for the conformal simulation was selected as 50% to ensure that the number of time iterations was not exceedingly high. Figure 10 shows the staircased and conformal discretization of the joint of the flip phone.

The conformal simulation with 2.8million cells is compared to a fine staircased simulation with 12.1million cells. The simulation time was 81minutes for the conformal run and 277 minutes for the staircased run on an Intel P4, 2.7GHz. The near field RMS |E| was plotted on a plane 5mm below the lowest point of the antenna. In Figure 11 the contour plots of that plane are shown. Along the bright line the relative error L_2 of the conformal simulation compared to the fine reference one is only 2.4%, regarding the reduced computational resources achieved. Small deviations are also obtained observing the feedpoint impedance which changes from $45.8 + j 1.07 \Omega$ to $45.6 - j 1.45 \Omega$ for conformal and fine simulation, respectively.

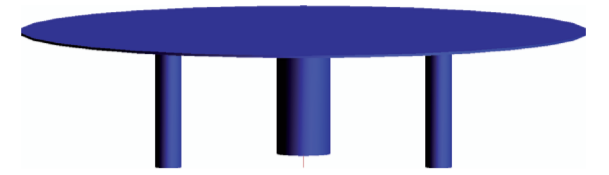


Figure 8: The CAD model of the broadband low profile antenna is shown. The excitation (small line) is between the center rod and the PEC ground plane. The ground plane is not drawn in the picture.

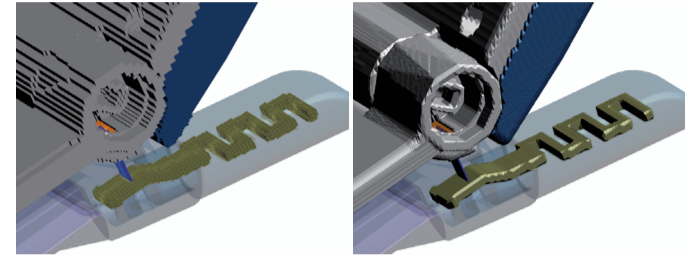


Figure 10: The joint of a flip phone staircased (left) and conformally (right) voxelized.

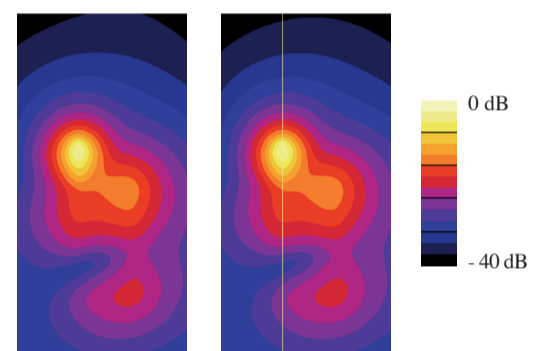


Figure 11: The RMS value of the absolute E field is shown for the conformal simulation (left) and the fine reference staircase simulation (right).

CONCLUSIONS

The major new contributions on the conformal FDTD updating scheme can be summarized as follows:

- less memory consumption than [2,3]
- less multiplications per time step than [2,3]
- conventional update equation, but conformally enhanced update coefficients
- derived stability criterion
- which allows the user to favor either speed or accuracy
- straight forward adaptation to hardware accelerated and/or parallelized FDTD codes, because of conventional update equations

The novel proposed and implemented conformal meshing algorithms and the locally conformal FDTD scheme enable improved spatial modeling and simulation of complex 3-D real-world structures. They were validated on the basis of benchmark examples as well as targeting complex industrial applications. The new methods constitute a significant benefit and performance increase for electromagnetics related applications in general and for mobile communication and medicine in particular. With them, CAD datasets from industrial environments can be imported and reliably meshed within a few minutes. Moreover, the new 3-D conformal scheme demonstrated orders of magnitude in reduction of computational runtime and memory requirements, by maintaining the same order of accuracy.

ACKNOWLEDGMENTS

This study was generously supported by the Swiss Commission for Technology and Innovation (CTI) and Schmid & Partner Engineering AG (SPEAG).

REFERENCES

- [1] Allen Taflove and Susan Hagness, Computational Electrodynamics: The Finite-Difference Time-Domain Method, 2 ed., Artech House, Boston, MA, 2000.
- [2] S. Dey and R. Mittra, A Modified Locally Conformal Finite-Difference Time-Domain Algorithm for Modeling Three-Dimensional Perfectly Conducting Objects, Microwave and Optical Technology Letters, vol. 17, no. 6, 349-352, April, 1998.
- [3] W. Yu and R. Mittra, A Conformal FDTD Algorithm for Modeling Perfectly Conducting Objects with Curve-Shaped Surfaces and Edges, Microw. Opt. Technol. Lett., vol. 27, no. 2, pp. 136-138, Oct. 2000.
- [4] T. Xiao and Q. H. Liu, Enlarged cells for the conformal FDTD method to avoid the time step reduction, IEEE Microwave and Wireless Components Letters, vol. 14, no. 12, pp. 551-553, December 2004.
- [5] SEMCAD X: www.semcad.com
- [6] T. Su, Y. Liu, W. Yu, and R. Mittra, A Conformal Mesh-Generating Technique for the Conformal Finite-Difference Time-Domain (CFDTD) Method, IEEE Antennas and Propagation Magazine, vol. 46, no. 1, 37-49, February, 2004.
- [7] S. Benkler, N. Chavannes, and N. Kuster, A New 3-D Conformal PEC FDTD Scheme With User-Defined Geometric Precision and Derived Stability Criterion, IEEE Trans. Ant. Prop., vol. 54, no. 6, pp. 1843-1849, 2006.